UMYU Scientifica, Vol. 3 NO. 1, March 2024, Pp 225 – 234
https://doi.org/10.56919/usci.2431.025
ISSN: 2955 – 1145 (print); 2955 – 1153 (online)
A periodical of the Faculty of Natural and Applied Sciences, UMYU, Katsina

ORIGINAL RESEARCH ARTICLE

Geophysical Evaluation of Subsurface Geology for Foundation Purposes at Wukari, Northeastern Nigeria, Using Electrical Resistivity Method

Ahmed Ibrahim Isiaka[1]*, Byami Andrew Jolly[1], Abubakar Rabiu[1], Umaru Aliyu Ohiani[2], and Abdulmalik Nana Fatima[3].

[1]Department of Geology, Ahmadu Bello University Zaria, Nigeria.
[2]Department of Geology, University of Maiduguri, Nigeria.
[3]Center for Energy Research and Training, Ahmadu Bello University Zaria, Nigeria.

ABSTRACT

Geophysical investigation using the electrical resistivity method was conducted at a proposed engineering site in Wukari, northeastern Nigeria, to evaluate the subsurface geology for foundation purposes. The main objective of the investigation was to delineate the subsurface stratigraphy and the geological structures beneath the study area that may influence the safe development of the proposed site. Vertical electrical sounding (VES) surveying technique, which utilizes the Schlumberger electrode array, was employed to acquire 1D resistivity data at 40 stations in the area. The data were acquired at regular station intervals of 100 m along four profiles, including three East-West parallel profiles and a perpendicular North-South profile of approximately 1 km each in length. The survey revealed the study area to be underlain by three stratigraphic units, comprising (1) clayey-sand to lateritic topsoil with an average resistivity of 1750 Ωm and thickness of about 12 m, (2) a middle layer, predominantly clay/shale, with an average resistivity of 28 Ωm and thickness that increases from approximately 20 m in the south to about 100 m towards the north, and (3) a moderately to highly indurated sandstone bedrock that dips at approximately 20 degrees to the north and characterized by high resistivity values with an average of 3414 Ωm. The survey also revealed the overburden thickness to be increasing from about 35 m in the south of the study area to about 100 m in the north, while near-surface structures such as fold, fault and fractures that can influence the safe development of the proposed site were also detected beneath the study area.

ARTICLE HISTORY

Received December 14, 2023.
Accepted March 21, 2024.
Published March 30, 2024.

KEYWORDS

Wukari; Resistivity; Foundation; VES; Benue Trough

INTRODUCTION

Subsurface investigation prior to the construction of engineering structures is very important to the safe development of an engineering site. Besides providing information about the subsurface geological conditions that may influence engineering structures, information derived from such investigation is essential to engineers deciding the design mode and the foundation to be employed in any civil engineering project. One of the paramount objectives of conducting the subsurface investigation for civil works is to adequately understand the disposition of subsurface geological structures (e.g. faults, folds, joints and fractures) and rock strata beneath a site, especially if such site is located in a complex geological terrain. To achieve this important objective, near-surface applications of non-invasive geophysical methods are now effectively employed in engineering site investigation that requires high-resolution imaging of near-surface geological features (Isiaka et al., 2018; Abubakar et al., 2019; Hassan et al., 2020). Geophysical methods are relatively cheap, nondestructive and time-effective when compared to the traditional sampling by drilling, and their dependent on the contrast in the physical properties of earth materials makes them suitable for obtaining accurate information about the subsurface (Loke et al., 2007; Jardani et al. 2009; Chambers et al. 2015).

Geophysical methods, including gravity, magnetic, seismic, and electrical methods, have been successfully employed in subsurface investigation for environmental and civil engineering works (e.g. Breytenbach and Bosch, 2011; Francke, 2016; Isiaka et al., 2018). Among these geophysical methods, the electrical resistivity method is the most frequently used in engineering site investigation because it is relatively cheap, efficient and convenient. The

Correspondence: Ahmed Ibrahim Isiaka. Department of Geology, Ahmadu Bello University Zaria, Nigeria. ✉ ahmedish002@gmail.com.

How to cite: Isiaka, A. I., Byami, A. J., Abubakar, R., Umaru, A. O., & Abdulmalik, N. F. (2024). Geophysical Evaluation of Subsurface Geology for Foundation Purposes at Wukari, Northeastern Nigeria, Using Electrical Resistivity Method. *UMYU Scientifica*, 3(1), 225 – 234. https://doi.org/10.56919/usci.2431.025

method depends on the contrast in the electrical resistivity among earth materials and can be used to produce accurate data on the lateral and vertical variation of geological materials in the shallow subsurface. Generally, the technique is based on the surface measurements of the potential difference caused by introducing electric currents through the subsurface. It is extensively used in groundwater exploration to delineate subsurface water-bearing aquifers (e.g. Goldman and Neubauer, 1994; Adepelumi et al., 2013; Bhadra et al., 2021; Wahab et al., 2021) and in environmental and engineering works to evaluate subsurface geological conditions for foundation purposes (e.g. Van Schoor, 2002; Abubakar et al., 2020; Bomi et al., 2020; Hassan et al., 2020).

This study used the electrical resistivity method to conduct a subsurface investigation at a proposed engineering site at the Federal University Wukari in Taraba State, northeastern Nigeria. The main aim of the investigation was to properly evaluate the subsurface geological conditions beneath the proposed site for foundation purposes, with the objectives of delineating the subsurface stratigraphy and the near-surface geological structures that may influence the safe development of the site.

Location and Geology of the Study Area

The study area is a proposed engineering site located at Wukari in Taraba State, northeastern Nigeria, and bounded by latitudes: 07^0 50' 25.2" N, 07^0 51' 06.50" N and longitudes: 009^0 45' 51.12" E, 009^0 46' 46.48" E (Figure 1). The proposed site covers an area of about 1.96 sq. km and is generally characterized by a flat topography.

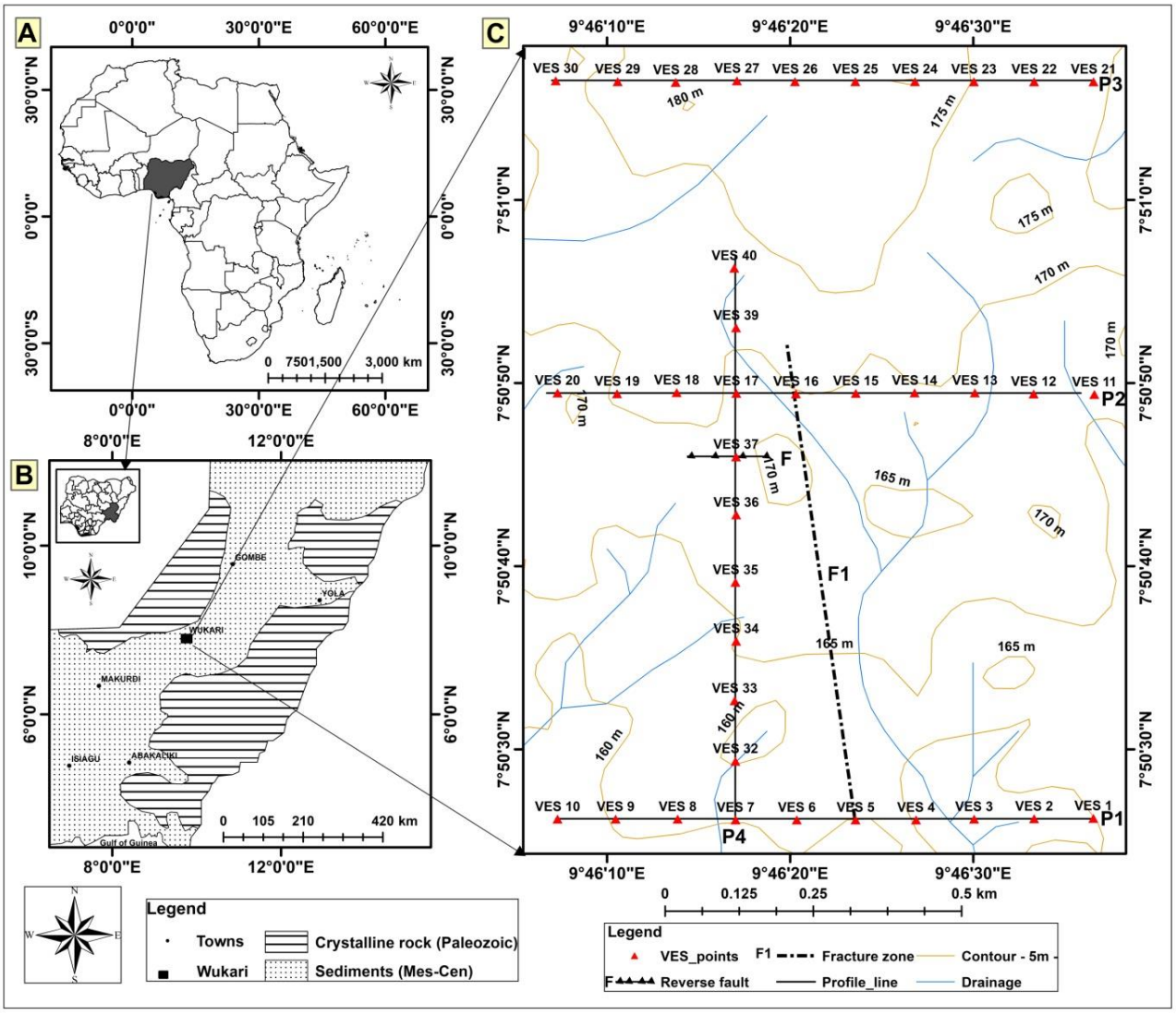

Figure 1: (A) Map of Africa showing the outline of Nigeria, (B) Geological map of Benue Trough (modified from Benkhelil, 1989) showing the approximate location of the study area, and (C) the Topographic map of the study area showing the VES stations and the profiles acquired in the area, as well as the location of the suspected reverse fault and the fracture zones detected beneath the study area.

Wukari is regionally located within the Cretaceous sedimentary basin of the Middle Benue Trough of Nigeria (Figure 1), which is a rifted trough that developed as a result of the separation between Africa and the South

America continent (Benkhelil, 1989). The Benue Trough's tectonic evolution has been characterized by deformational processes involving extensional faulting, strike-slip faulting and associated trans-pressional folding (Benkhelil, 1989; Guiraud, 1993). This is evident by the widespread occurrence of deformational structures such as large- to small-scale normal faults, reverse faults, folds, transcurrent shear zones, and shear fractures documented from the basin (Benkhelil, 1989). The notable tectonic episode in the Benue Trough occurred during the Santonian compression, where folding was the dominant deformational process (Benkhelil, 1989). In the Middle Benue Trough, where the study area is located, the Santonian compression produced folds of different styles and attitudes on all scales, from a few centimeters microfolding to several kilometers long anticlines and synclines (Benkhelil, 1989). The study area is stratigraphically underlain by the sediments of the Awe Formation that were deposited during the Late Albian to Early Cenomanian marine regression. The deposits are estimated to be about 1000 m thick (Offodile, 1976) and consist of medium- to coarse-grain calcareous sandstones, shales, and clays. The lateritic soil derived from the weathering of the underlying clays is commonly seen in the study area, forming the topsoil.

METHODOLOGY

The principle of the electrical resistivity method is based on Ohm's Law. It involves the injection of electric current (I) into the ground through a pair of electrodes. At the same time, the resulting potential difference or voltage (V) at the surface is measured through another pair of electrodes. The ratio of the potential difference (V) measured at the potential electrodes to the input current (I) at the current electrodes gives the resistance (R) (Eq. 1), which represents the impedance of the subsurface geological layers. Different linear electrode array configurations can be employed to obtain the resistivity (ϱ) of subsurface earth materials. Commonly used array configurations in the electrical resistivity method are the Schlumberger, Wenner, and the Dipole-dipole electrode array, with varied depth of investigation and resolution capacity. The subsurface resistivity is achieved by multiplying the measured resistance (R) by a geometric factor (K) that is determined from the electrode arrangement (Eq. 2).

$$R = \frac{V}{I} \quad (1)$$

$$\varrho = K.\frac{V}{I} \quad (2)$$

In an inhomogeneous or horizontally layered earth, the resistivity obtained from Eq. 2 is an apparent resistivity (ϱ_a) and depends on the contribution from the resistivity of the different surrounding geological units and the electrode spacing.

The vertical electrical sounding (VES) surveying technique that utilizes the Schlumberger electrode configuration was employed in this investigation (Figure 2). The field practice of this technique requires four electrodes with two inner potential electrodes (M and N) and two outer current electrodes (A and B) that are coaxially arranged about a fixed central point. The initial set out of the Schlumberger array usually begins with a short electrode separation of AB/2 of 1.5 m, followed by a progressive expansion of the current electrodes at intervals to about 100 m or more relative to the mid-point. This progressive increase in the distance between the current electrodes results in greater penetration depth and probing by the current.

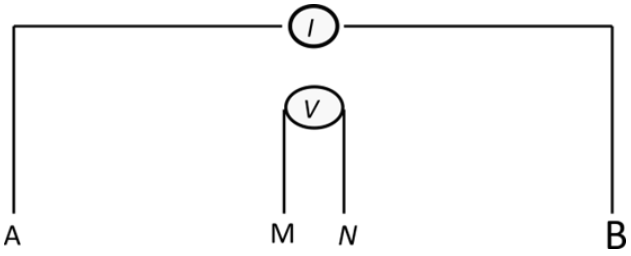

Figure 2: An illustration of the Schlumberger array configuration employed in this investigation.

Data Acquisition

Using the Schlumberger electrode configuration, 1D vertical electrical sounding (VES) data were acquired at 40 stations in the study area with the aid of an Ohmega resistivity meter. The VES data were acquired along four (4) profiles of approximately I km each. Three of these profiles (P1, P2, and P3) were acquired parallel to each other and run from east to west, while the fourth profile (P4) runs perpendicularly from south to north (Figure 1). In order to achieve an appreciable depth of investigation and proper lateral correlation, the survey utilized maximum current electrodes separation of 200 m at stations spaced at intervals of 100 m along each profile. Similarly, to generate a subsurface 2D pseudo-section, the same current azimuth was maintained at each station along the profiles throughout the data acquisition. This is based on the assumption that subsurface vertical geological structures such as faults, folds or fractures, usually characterized by lateral layer discontinuities, can cause anomalous distortions in current flow lines that may indicate their presence.

Data Processing

The VES data acquired in the study area during the field campaign were processed using the Ipi2Win resistivity software package. The resistance obtained from the resistivity meter at each VES station was converted to apparent resistivity after multiplying by the corresponding geometric factor determined for each successive electrode spacing. This was followed by the generation of 1D VES curves from the plot of the apparent resistivity values against the electrode spacing (AB/2) and the matching of the apparent resistivity curves. The 1D inversion process, aimed at minimizing the difference between the measured resistivities and the calculated response of the estimated model, was later applied to the data. This was carried out

through a number of iteration steps until a satisfactory agreement was reached between the calculated model and the field data. Subsequent 1D inverted models obtained at each station along the profiles (Figure 3) were then concatenated to produce a 2D pseudo-section of the subsurface along each profile (Figures 4a, 5a, 6a, and 7a). The final processing step applied to the data was the lateral correlation of the resistivity sections derived from the inverted models (Figure 4b, 5b, 6b, and 7b) and the generation of a 2D geo-electrical model that best represents the subsurface geology below each profile (Figure 4c, 5c, 6c, and 7c).

RESULTS AND DISCUSSION

The rare occurrence of outcrops or geological sections of the underlying bedrock and the lack of borehole data make it difficult to properly constrain the interpretation of the results obtained from the study area. Hence, the interpretation of the results was based on the general knowledge of the regional geology of the area (see Offodile, 1976 and Benkhelil, 1989) and the inferences derived from the observed resistivity values (Table 1). The initial correlation of the inverted models generally shows similar curve styles that indicate uniform subsurface stratigraphic units with varied layer thickness along the profiles (Figure 3). As inferred from the resistivity values, the 2D geo-electrical models obtained for all the profiles indicate three subsurface stratigraphic units (Figure 4, 5, 6 & 7). These units consist of the topsoil (made up of clayey sand or lateritic soil) with resistivity values that vary from 60 Ωm to about 5800 Ωm and an average thickness of about 12 m; the middle layer, which is probably made up of shale or clay with resistivity values that range from 7 Ωm to about 53 Ωm and the thickness that increases from about 20 m in the south to about 100 m towards the north; and the bedrock suspected to be moderate to highly indurated sandstone with resistivity values that range from about 550 Ωm to about 7000 Ωm.

The geo-electrical sections obtained along the profiles indicate the possible existence of near-surface geological structures beneath the proposed site. The characteristic undulation of the underlying bedrock, which is suspected to have resulted from folding, is noticeable in the E-W sections (Figure 4c, 5c, and 6c), as well as in the perpendicular section (profile P4), where the suspected sandstone bedrock is seen to be dipping at approximately 20 degrees towards the north (Figure 7c). This also implies that the overburden thickness in the study area is not uniform but varies from approximately 35 m in the south to about 100 m in the north. Similarly, near-surface evidence of the existence of a fault is revealed along profile P4 (Figure 7c), where possible reverse faulting is seen to have caused a lateral discontinuity observed in the pseudosection and the geo-electrical section below profile P4 (Figure 7b and 7c). In addition, an anomalous zone characterized by low resistivity values of less than 120 Ωm is also observed within the underlying bedrock below profiles P1 and P2 (Figure 4c and 5c, respectively). This zone is interpreted as a possible fracture zone that may have resulted from shearing or faulting along a NNW-SSE trend (Figure 1).

Subsurface discontinuities like faults and fractures detected beneath the study area can pose a hazard to the safe development of the area. These geological structures tend to permit sliding of the foundation that may result in the failure of engineering structures, and may have to be avoided during construction. Similarly, the non-uniformity of the thickness of the clay overburden, as observed in the area, can cause differential settlement that may lead to tilting and the eventual breaking of the building. Therefore, appropriate foundations must be employed during construction to avoid the future failure of the engineering structures in the study area.

Table 1: The resistivity values and the inferred stratigraphic units obtained below each station after the inversion processes

VES Stations	Layer	Resistivity (Ohm-m)	Inferred Geology
VES01	1	742	Lateritic soil
	2	60.6	Clayey-sand
	3	8.44	Clay/Shale
	4	641	Sandstone
VES02	1	291	Lateritic soil
	2	14.9	Clay/Shale
	3	5755	Sandstone
VES03	1	226	Lateritic soil
	2	176	Clayey-sand
	3	3.29	Clay/Shale
	4	4190	Sandstone
VES04	1	533	Lateritic soil
	2	246	Clayey-sand
	3	21.4	Clay/Shale
	4	4319	Sandstone
VES05	1	203	Lateritic soil

	2	84	Clayey-sand
	3	4.43	Clay/Shale
	4	137	Sandstone
VES06	1	227	Lateritic soil
	2	13.5	Clay/Shale
	3	1214	Sandstone
VES07	1	436	Lateritic soil
	2	69.4	Clayey-sand
	3	11.2	Clay/Shale
	4	1310	Sandstone
VES08	1	302	Lateritic soil
	2	138	Clayey-sand
	3	10.3	Clay/Shale
	4	5602	Sandstone
VES09	1	1475	Lateritic soil
	2	93.8	Clayey-sand
	3	10.9	Clay/Shale
	4	3691	Sandstone
VES10	1	670	Lateritic soil
	2	1665	Laterite
	3	43	Clay/Shale
	4	845	Sandstone
VES11	1	390	Lateritic soil
	2	78	Clayey-sand
	3	16.1	Clay/Shale
	4	5523	Sandstone
VES12	1	261	Lateritic soil
	2	3421	Laterite
	3	69.2	Clayey-sand
	4	25.7	Clay/Shale
	5	1466	Sandstone
VES13	1	619	Lateritic soil
	2	1370	Laterite
	3	17.4	Clay/Shale
	4	2850	Sandstone
VES14	1	491	Lateritic soil
	2	5396	Laterite
	3	216	Clayey-sand
	4	20.4	Clay/Shale
	5	4661	Sandstone
VES15	1	493	Lateritic soil
	2	76.6	Clayey-sand
	3	25.7	Clay/Shale
	4	7612	Sandstone
VES16	1	298	Lateritic soil
	2	145	Clayey-sand
	3	9.5	Clay/Shale
	4	119	Sandstone
VES17	1	521	Lateritic soil
	2	102	Clayey-sand
	3	17.7	Clay/Shale
	4	2410	Sandstone
VES18	1	759	Lateritic soil
	2	355	Clayey-sand
	3	28.6	Clay/Shale
	4	3714	Sandstone
VES19	1	590	Lateritic soil

	2	62.9	Clayey-sand
	3	23.5	Clay/Shale
	4	4997	Sandstone
VES20	1	437	Lateritic soil
	2	206	Clayey-sand
	3	29	Clay/Shale
	4	774	Sandstone
VES21	1	866	Lateritic soil
	2	5439	Laterite
	3	93.5	Clayey-sand
	4	23.6	Clay/Shale
	5	7403	Sandstone
VES22	1	938	Lateritic soil
	2	4907	Laterite
	3	240	Clayey-sand
	4	23.9	Clay/Shale
	5	5535	Sandstone
VES23	1	848	Lateritic soil
	2	18.7	Clay/Shale
	3	2343	Sandstone
VES24	1	1328	Laterite
	2	418	Clayey-sand
	3	20.2	Clay/Shale
	4	4791	Sandstone
VES25	1	1751	Laterite
	2	176	Clayey-sand
	3	30.9	Clay/Shale
VES26	1	874	Laterite
	2	24.1	Clay/Shale
	3	1503	Sandstone
VES27	1	466	Lateritic soil
	2	245	Lateritic soil
	3	147	Clayey-sand
	4	47.2	Clay/Shale
VES28	1	278	Lateritic soil
	2	72.4	Clayey-sand
	3	36.5	Clay/Shale
VES29	1	396	Lateritic soil
	2	97.4	Clayey-sand
	3	25.7	Clay/Shale
	4	3454	Sandstone
VES30	1	436	Lateritic soil
	2	1516	Laterite
	3	33.5	Clay/Shale
VES31	1	436	Lateritic soil
	2	65.4	Clayey-sand
	3	11.5	Clay/Shale
	4	1310	Sandstone
VES32	1	536	Lateritic soil
	2	212	Clayey-sand
	3	7.32	Clay/Shale
	4	1864	Sandstone
VES33	1	456	Lateritic soil
	2	27.9	Clay/Shale
	3	1107	Sandstone
VES34	1	447	Lateritic soil
	2	24.9	Clay/Shale

	3	1855	Sandstone
VES35	1	259	Lateritic soil
	2	1018	Laterite
	3	37.5	Clayey-sand
	4	9.43	Clay/Shale
	5	1929	Sandstone
VES36	1	617	Laterite
	2	307	Lateritic soil
	3	72.4	Clayey-sand
	4	24.1	Clay/Shale
VES37	1	456	Lateritic soil
	2	41.8	Clay/Shale
	3	92.2	Clayey-sand
VES38	1	521	Lateritic soil
	2	102	Clayey-sand
	3	17.7	Clay/Shale
	4	2410	Sandstone
VES39	1	436	Lateritic soil
	2	36.3	Clay/Shale
	3	29.7	Clay/Shale
VES40	1	576	Lateritic soil
	2	53.9	Clayey-sand
	3	35.3	Clay/Shale

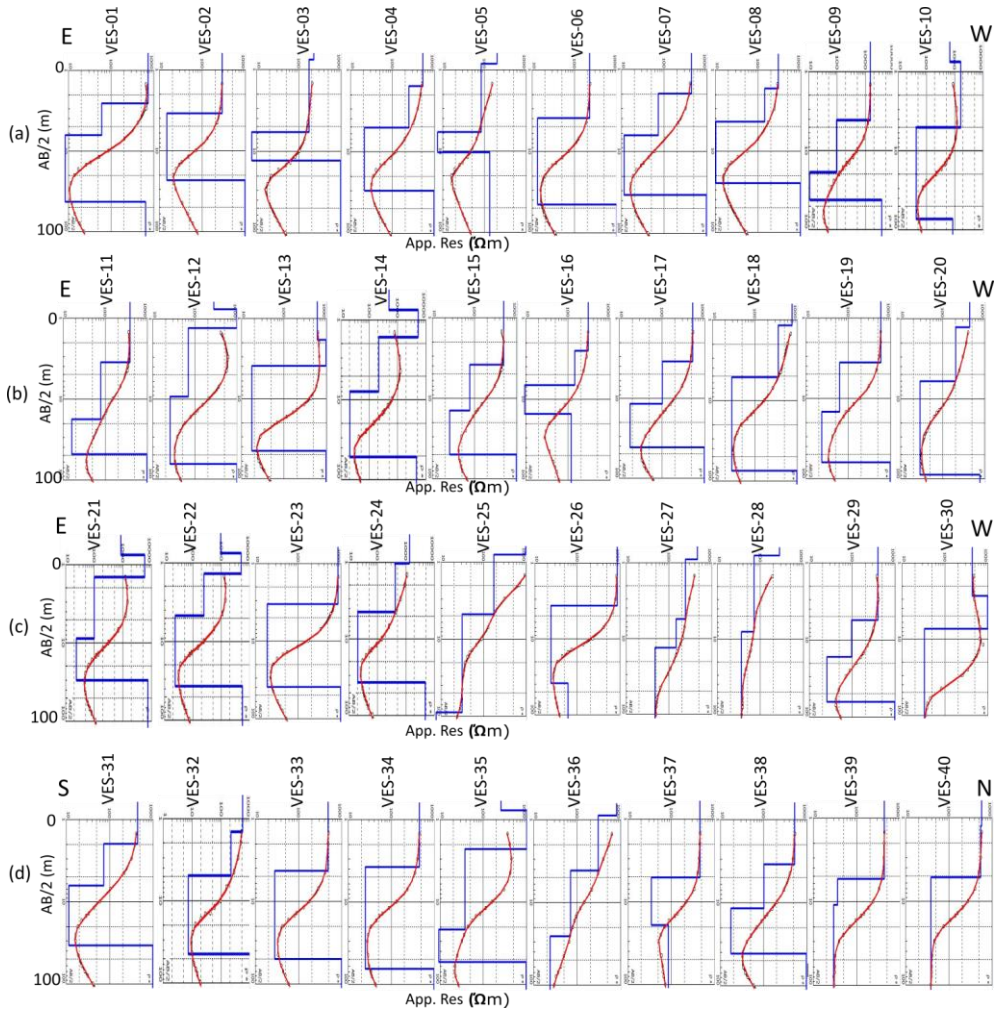

Figure 3: Lateral correlation of all the VES curves obtained after the inversion along profile (a) P1, (b) P2, (c) P3, and (d) P4

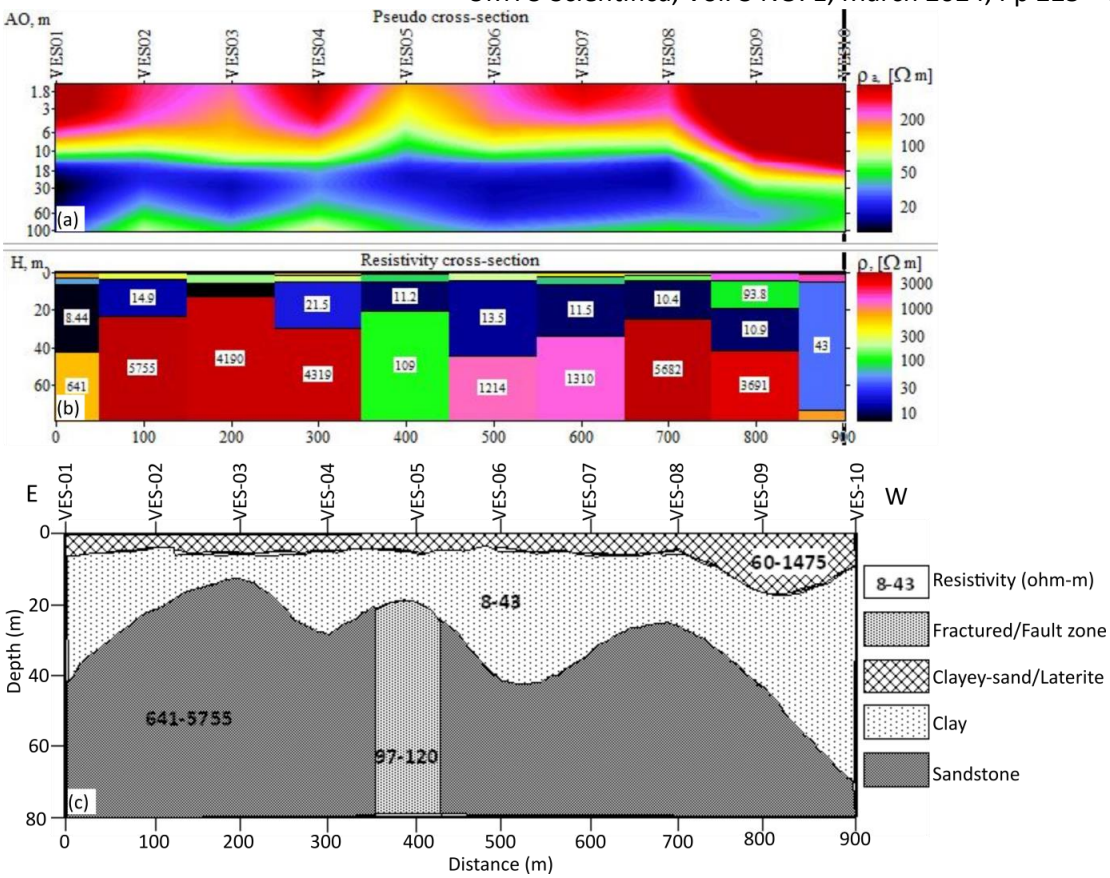

Figure 4: (a) The pseudosection, (b) the resistivity section, and (c) the geo-electrical section obtained along profile P1. Note the suspected fracture zone within the bedrock beneath station VES05.

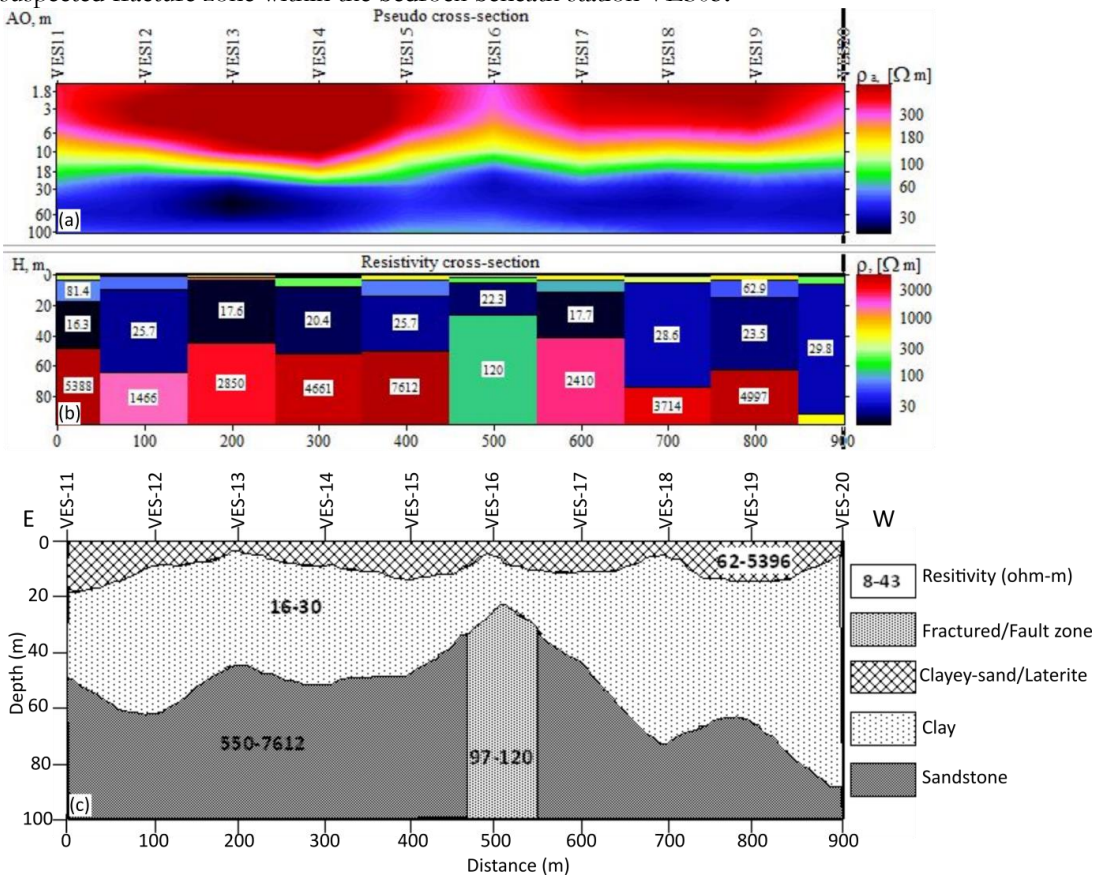

Figure 5: (a) The pseudosection, (b) the resistivity section, and (c) the geo-electrical section obtained along profile P2. Note the suspected fracture zone within the bedrock beneath station VES16.

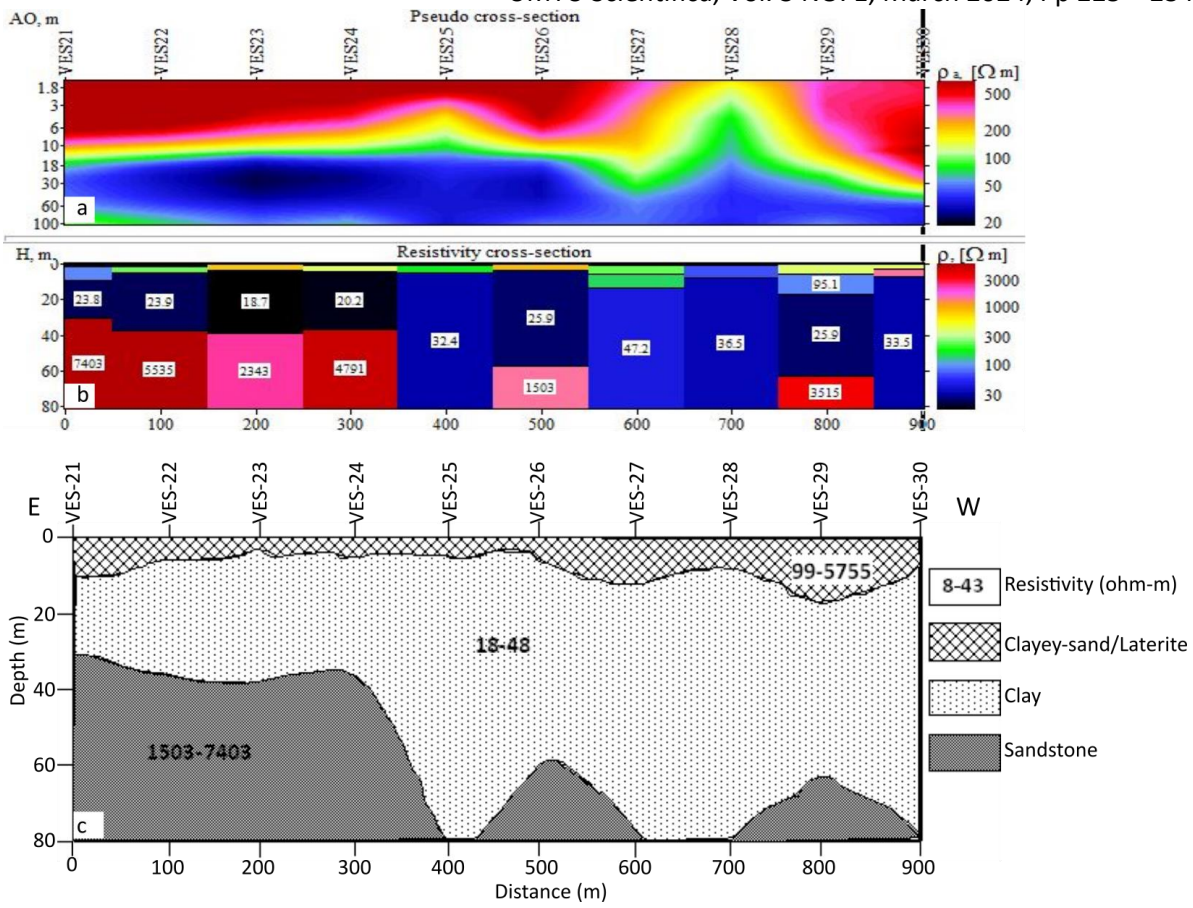

Figure 6: (a) The pseudosection, (b) the resistivity section, and (c) the geo-electrical section obtained along profile P3.

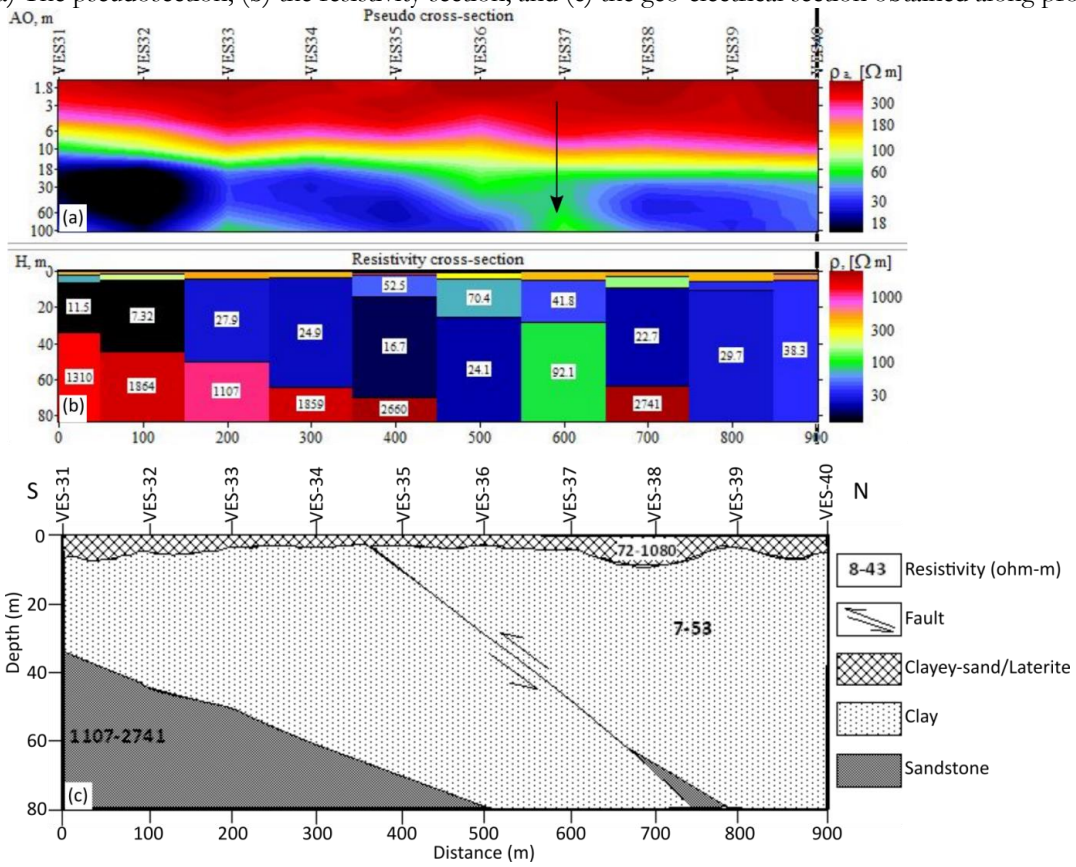

Figure 7: (a) The pseudosection, (b) the resistivity section, and (c) the geo-electrical section obtained along profile P4. Note the arrow indicating the lateral layer discontinuity caused by the suspected reverse fault beneath the profile

CONCLUSIONS

This investigation has revealed the study area to be underlain by three stratigraphic units, which include a clayey-sand to lateritic topsoil with an average resistivity of 1750 Ωm and average thickness of about 12 m, clay/shale layer with thickness that increases from about 20 m in the south to about 100 m towards the north and average resistivity value of 28 Ωm, and a moderate to highly indurated sandstone bedrock that dips at approximately 20 degrees towards the north and characterized by high resistivity values with an average of 3414 Ωm. Similarly, the overburden thickness is also revealed by this investigation to increase from about 35 m south of the study area to about 100 m north. In addition, near-surface structures such as folds, faults and fractures that exist beneath the study area were also delineated. These structures can influence the safe development of the proposed site and may have to be avoided, or an appropriate foundation should be employed during construction to avoid the future failure of engineering structures in the area.

ACKNOWLEDGEMENT

The author would like to thank the management of TECTONICS Engineering Consults, Maitama Abuja, Nigeria, for permitting us to publish the data used in this study. Our appreciation also goes to the two anonymous reviewers for their contributions, which have helped improve the quality of this manuscript.

REFERENCES

Abubakar F., Ahmed. I. I., Aminu, A. L., and Lawal K. M., (2019). 1-Dimensional shear wave velocity analysis of the phase II site, Ahmadu Bello University Zaria, using Multichannel Analysis of Surface Wave (MASW). *FUDMA Journal of Sciences,* 3(3), 436-443.

Abubakar, F., Ahmed, I. I., Idogbe, E. A., Usman, M.T. and Momoh, K.O. (2020). Site Characterization of the Proposed Agricultural Complex, Ahmadu Bello University, Zaria, Northern Nigeria, using Multi-Channel Analysis of Surface Waves. *Minna Journal of Geosciences,* 4, 2.

Adepelumi, A. A., Akinmade, O. B and Fayemi, O., (2013). Evaluation of Groundwater Potential of Baikin Ondo State Nigeria Using Resistivity and Magnetic Techniques: A Case Study. Universal Journal of Geoscience 1(2): 37-45. **[Crossref]**

Benkhelil, J., (1989). The Origin and Evolution of the Cretaceous Benue Trough (Nigeria). *Journal of African Earth Sciences (and the Middle East)*, 8, 251-282. **[Crossref]**

Bhadra, B.K., Gor, N., Jain, A.K., Meena, H., and Rao, S.S. (2021). Groundwater investigation of the artesian wells on the palaeochannels in parts of the Great Rann of Kachchh, Gujarat, India, using remote sensing and geophysical techniques. *Hydrogeology Journal, 29*, 2705 - 2724. **[Crossref]**

Bomi, L., Seokhoon, O., Myeong-Jong, Y., (2020). Mapping of leakage paths in damaged embankment using modified resistivity array method, *Engineering Geology,* 266, 105469, **[Crossref]**.

Breytenbach, I. J., and Bosch, P. J. A. (2011). Application, advantages and limitations of high-density gravimetric surveys compared with three-dimensional geological modeling in dolomite stability investigations. *Journal of the South African Institution of Civil Engineering*, 53, 7–11.

Chambers, J. E, Meldrum, P. I, Wilkinson, P. B., Ward, W, Jackson, C, Matthews, B, Joel, P, Kuras, O, Bai, L, Uhlemann, S, Gunn, D., (2015). Spatial monitoring of groundwater drawdown and rebound associated with quarry dewatering using automated time-lapse electrical resistivity tomography and distribution guided clustering. *Eng Geol* 193:412–420.. **[Crossref]**

Francke, J. (2016). Mapping paleochannels in the Libyan Sahara with ground penetrating radar. *2016 16th International Conference on Ground Penetrating Radar (GPR)*, 1-5. **[Crossref]**

Goldman, M. and Neubauer, F. (1994). Groundwater exploration using integrated geophysical techniques. *Surv. Geophys.* 15, 331–361. **[Crossref]**

Guiraud, M., (1993). Late Jurassic rifting–Early Cretaceous rifting and Late Creaceous transpressional inversion in the upper Benue Basin (NE Nigeria). Bull. De Centre des Recherches Exploration Production Elf – Aquitaine, 17, 371-383.

Hassan, M., Shang, Y., Jin, W., Akhter, G., (2020). An engineering site investigation using non-invasive geophysical approach. *Environ Earth Sci* 79, 265 . **[Crossref]**

Isiaka, A.I., Durrheim, R.J. and Manzi, M.S.D. (2018). High-resolution seismic reflection investigation of subsidence and sinkholes at an abandoned coal mine site in South Africa, *Pure and Applied Geophysics,* 176, 1531-1548. **[Crossref]**

Jardani, A., Revil, A,, Barrash, W. A., Crespy, E., Rizzo, S,, Straface, M., Cardiff, B., Malama, C., Miller, C, Johnson, T., (2009). Reconstruction of the water table from self potential data: a Bayesian approach. *Groundwater* 47:213–227. **[Crossref]**

Loke, M. H, Chambers, J. E, Rucker, D. F, Kuras, O., Wilkinson, P. B., (2013). Recent developments in the direct-current geoelectrical imaging method. *J Appl Geophys* 95:135–156. **[Crossref]**

Offodile, M. E. (1976). Review of the geology of the Cretaceous Benue Valley. In: Kogbe, C.A., Ed., Geology of Nigeria, *Elizabethan Publishing Coy, Lagos,* 319-330.

Van Schoor, M. (2002). Detection of sinkholes using 2D electrical resistivity imaging. *Journal of Applied Geophysics*, 50, 393–399. **[Crossref]**

Wahab, S., Saibi, H. and Mizunaga, H. (2021). Groundwater aquifer detection using the electrical resistivity method at Ito Campus, Kyushu University (Fukuoka, Japan). *Geosci. Lett.* 15. **[Crossref]**